THE JOURNAL OF BIOLOGICAL CHEMISTRY VOL. 283, NO. 34, pp. 23150–23160, August 22, 2008

Ric-8A Catalyzes Guanine Nucleotide Exchange on $G\alpha_{i1}$ Bound to the GPR/GoLoco Exchange Inhibitor AGS3*[S]

Received for publication, March 28, 2008, and in revised form, May 26, 2008 Published, JBC Papers in Press, June 9, 2008, DOI 10.1074/jbc.M802422200

Celestine J. Thomas[‡], Gregory G. Tall[§], Anirban Adhikari[¶], and Stephen R. Sprang[‡1]

From the [‡]Center for Bimolecular Structure and Dynamics and the Division of Biological Science, University of Montana, Missoula, Montana 59812, the [§]Department of Pharmacology and Physiology, University of Rochester Medical Center, Rochester, New York 14642, and the [¶]Department of Molecular Biology, University of Texas Southwestern Medical Center, Dallas, Texas 75390

Microtubule pulling forces that govern mitotic spindle movement of chromosomes are tightly regulated by G-proteins. A host of proteins, including Gα subunits, Ric-8, AGS3, regulators of G-protein signalings, and scaffolding proteins, coordinate this vital cellular process. Ric-8A, acting as a guanine nucleotide exchange factor, catalyzes the release of GDP from various Gα·GDP subunits and forms a stable nucleotide-free Ric-8A:Gα complex. AGS3, a guanine nucleotide dissociation inhibitor (GDI), binds and stabilizes Gα subunits in their GDP-bound state. Because Ric-8A and AGS3 may recognize and compete for Gα·GDP in this pathway, we probed the interactions of a truncated AGS3 (AGS3-C; containing only the residues responsible for GDI activity), with Ric-8A:$G\alpha_{i1}$ and that of Ric-8A with the AGS3-C:$G\alpha_{i1}$·GDP complex. Pulldown assays, gel filtration, isothermal titration calorimetry, and rapid mixing stopped-flow fluorescence spectroscopy indicate that Ric-8A catalyzes the rapid release of GDP from AGS3-C:$G\alpha_{i1}$·GDP. Thus, Ric-8A forms a transient ternary complex with AGS3-C:$G\alpha_{i1}$·GDP. Subsequent dissociation of AGS3-C and GDP from $G\alpha_{i1}$ yields a stable nucleotide free Ric-8A·$G\alpha_{i1}$ complex that, in the presence of GTP, dissociates to yield Ric-8A and $G\alpha_{i1}$·GTP. AGS3-C does not induce dissociation of the Ric-8A·$G\alpha_{i1}$ complex, even when present at very high concentrations. The action of Ric-8A on AGS3:$G\alpha_{i1}$·GDP ensures unidirectional activation of Gα subunits that cannot be reversed by AGS3.

Canonical G-protein signaling pathways are activated when agonist-bound heptahelical receptors, acting as guanine nucleotide exchange factors (GEFs),[2] promote the exchange of GDP for GTP on Gα subunits present in Gα·GDP:Gβγ heterotrimers (1–3). Upon binding GTP, conformational changes in the switch regions of Gα subunits destabilize the heterotrimer and allow Gα·GTP to dissociate from Gβγ subunits (4, 5). Downstream regulatory molecules such as the regulators of G-protein signaling (RGS) accelerate Gα-catalyzed GTP hydrolysis, allowing the Gα subunits to revert to their resting GDP-bound conformation and priming them for the next receptor-induced G-protein cycle (6–8). Receptor-mediated signaling accounts for the majority of G-protein-regulated cellular control mechanisms. However, during the past few years evidence has emerged that, in both lower and higher eukaryotes, multicomponent G-protein signaling systems, operating outside the realm of membrane-bound receptors, play significant roles in various biological processes (9). These include control of the generation of microtubule pulling forces during cell division (10–16), synaptic signaling processes (17), and cardiovascular function (18). A receptor-independent G-protein-mediated signaling pathway, regulating a fundamental event such as asymmetric cell division, may involve proteins that can modulate G-protein nucleotide exchange in a manner that resembles the action of agonist-bound receptors and Gβγ subunits.

In nematodes, asymmetric cell division is a result of eccentric positioning of the mitotic spindle apparatus and the generation of cortical pulling forces on the posterior spindle poles by astral microtubules (13). Studies of fertilized eggs from *Caenorhabditis elegans* show that mutational inactivation of Gα subunits GOA-1 and GPA-16 leads to defective astral microtubule motion, indicating that these two proteins are vital for the proper positioning of the mitotic spindle (19–21). Along with Gα subunits, GPR1/2 proteins that contain GoLoco/G protein regulatory (GPR) motifs, operating in conjunction with "resistance to inhibitors of cholinesterase" (Ric-8) and RGS7, are necessary and sufficient for regulation of these events (22–27). In dividing *Drosophila* neuroblasts, $G\alpha_i$ subunits complexed with the GPR/GoLoco motif-containing protein PINS (PINS indicates Partner of Inscuteable) binds to Inscuteable or MUD to control asymmetric cell division (28, 29). In dividing sensory precursor cells of *Drosophila*, Ric-8 has been shown to positively regulate $G\alpha_i$ activity and is implicated in the membrane targeting of both PINS and $G\alpha_i$ subunits (29–31). Biochemical characterization of Ric-8 and GPR/GoLoco motif proteins indicate that they respectively exhibit GEF and guanine nucleotide dissociation inhibitory (GDI) activity toward Gα.

The mammalian 60-kDa protein Ric-8A, identified as a Gα-binding protein by yeast two-hybrid analysis, has been

* This work was supported, in whole or in part, by National Institutes of Health Grants R01-DK46371 (to S. R. S.) and GM34497 (to Alfred G. Gilman). The costs of publication of this article were defrayed in part by the payment of page charges. This article must therefore be hereby marked "*advertisement*" in accordance with 18 U.S.C. Section 1734 solely to indicate this fact.

[S] The on-line version of this article (available at http://www.jbc.org) contains supplemental Figs. 1 and 2.

[1] To whom correspondence should be addressed. Tel.: 406-243-6028; E-mail: stephen.sprang@umontana.edu.

[2] The abbreviations used are: GEF, guanine nucleotide exchange factor; AGS, activator of G-protein signaling; Ric-8A, resistance to inhibitors of cholinesterase 8A; GPR, G-protein regulatory motif; RGS, regulators of G-protein signaling; NuMA, nuclear mitotic apparatus protein; GDI, guanine nucleotide dissociation inhibitor; GTPγS, guanosine 5′-[γ-thio]triphosphate; PMSF, phenylmethanesulfonyl fluoride; GST, glutathione *S*-transferase; TEV, tobacco etch virus; IMAC, immobilized metal ion affinity chromatography; CFP, cyan fluorescent protein; YFP, yellow fluorescent protein; FRET, fluorescence resonance energy transfer; DTT, dithiothreitol; FPLC, fast protein liquid chromatography; ITC, isothermal titration calorimetry.

shown *in vitro* to bind to resting state (GDP-bound) $G\alpha_{i1}$, $G\alpha_q$, and $G\alpha_o$ and catalyze the exchange of GDP for GTP (and slowly hydrolyzing analogs of GTP) (32). Ric-8A forms a stable complex with nucleotide-free $G\alpha_{i1}$ that dissociates in the presence of GTP, releasing $G\alpha_{i1}$·GTP (32). Although the action of Ric-8A on $G\alpha$ subunits resembles that of a G-protein-coupled receptor, Ric-8A does not directly compete with the receptor for $G\alpha_{i1}$·GDP as it does not recognize $G\alpha_{i1}$·GDP in a $G\beta\gamma$-bound heterotrimeric state (32). However, human embryonic kidney cells (292T) transfected with Ric-8A-specific short interfering RNA exhibited a suppression of $G\alpha_q$-coupled/receptor-mediated extracellular signal-regulated kinase (ERK) activation, indicating that Ric-8A may also potentiate $G\alpha_q$-mediated signaling (33).

A recently identified class of regulators, typified by "activator of G-protein signaling 3" (AGS3), which bears four GPR/GoLoco signature motifs, has been shown to possess GDI activity similar to that of $G\beta\gamma$ subunits (34–38). The N-terminal portion of AGS3 consists of seven tetratricopeptide repeats that are implicated in cellular trafficking of protein binding partners (34, 35). An N-terminally truncated variant of AGS3 produced by alternative or trans-mRNA splicing, comprising only the GPR/GoLoco motifs of AGS3, has been found in mammalian heart (39). This variant of AGS3 possesses the C-terminal three GPR/GoLoco motifs but encodes only half of the first GPR/GoLoco motif present in the full-length AGS3. For this work, we have used a synthetic short form of AGS3 (AGS3-C) that encodes all four GPR/GoLoco motifs (35). Earlier thermodynamic studies have shown that all four GPR/GoLoco motifs of AGS3-C bind cooperatively to $G\alpha_{i1}$·GDP and form a stable AGS3-C:$[G\alpha_{i1}\cdot GDP]_4$ complex (40). For simplicity, we henceforth refer to this complex as AGS3-C:$G\alpha_{i1}$·GDP. The structure of the complex between the GPR/GoLoco peptide of RGS14 and $G\alpha_{i1}$·GDP reveals that GPR/GoLoco motifs function as GDIs by interacting with the switch II regions and the α3 helix of the $G\alpha_{i1}$ Ras-like domain (41). The arginine residue located in the highly conserved Asp-Gln-Arg (DQR) triad in the GPR/GoLoco motif inserts into the GDP-binding site and interacts with the β-phosphate of GDP, thereby preventing the release of GDP from $G\alpha_{i1}$ subunits.

The interplay between the GEF activity of Ric-8A and the GDI effect of GPR/GoLoco proteins on $G\alpha$ subunits was recently demonstrated (42). LGN, a paralog of AGS3, and microtubule-binding nuclear mitotic apparatus protein (NuMA) were shown to interact with and stabilize $G\alpha_{i1}$·GDP in a $G\alpha_{i1}$·GDP:LGN:NuMA complex (43). The $G\alpha_{i1}$·GDP subunits in this complex are proposed to be substrates for the GEF activity of Ric-8A. Although this study provides evidence that Ric-8A forms a transient complex with $G\alpha_{i1}$·GDP:LGN:NuMA, it does not preclude the possibility that Ric-8A is a direct competitor of LGN for a common binding site on $G\alpha_{i1}$·GDP. These alternative models could have different implications for the roles of Ric-8A and GPR/GoLoco proteins in the putative receptor-independent regulatory events mediated by $G\alpha$ (42).

In this biophysical study we show that Ric-8A acts catalytically on $G\alpha_{i1}$·GDP complexed with AGS3-C to effect nucleotide exchange. We utilize fluorescence labeling and thermodynamic and enzyme kinetic analysis to show that Ric-8A forms a transient multimeric complex with AGS3-C:$G\alpha_{i1}$·GDP. This intermediate then decays to a stable, nucleotide-free Ric-8A·$G\alpha_{i1}$ heterodimer after liberating AGS3-C and GDP. The inhibitory effect of AGS3-C on the interaction between Ric-8A and $G\alpha_{i1}$·GDP is not strong enough to abrogate Ric-8A GEF activity. Further experiments indicate that AGS3-C cannot reassociate with the nucleotide-free Ric-8A·$G\alpha_{i1}$ complex, indicating that this reaction pathway proceeds in a unidirectional manner.

EXPERIMENTAL PROCEDURES

Molecular Cloning and Protein Expression—The open reading frame of rat Ric-8A, encoding amino acid residues 12–492 (Ric8-At), was amplified by PCR using attB-modified forward primer 5′-GGGGACAGTTTGTACAAAAAAGCAGGCTACGAAAACCTATACTTTCAGGGAGAGGAAGATGCGGTGACAGGA-3′ encoding a TEV site N-terminal to residue 12 and 3′-CACTTGTACAAACTGTTCGAGAGGTCCACTCTGGGTCGAAAGAACATGTTTCACCAGGGG-5′ as the reverse primer. The resulting PCR product was cloned into the pDEST-15 destination vector to be expressed as a GST fusion protein using the Gateway cloning system (Invitrogen). The expression vector was transformed into *Escherichia coli* Bl21(DE3)-RIPL cells and grown in LB media containing ampicillin (120 mg/liter) and induced with 300 μM of isopropyl β-D-thiogalactopyranoside at 20 °C. After overnight growth at 20 °C, cells were suspended in lysis buffer (50 mM Tris, pH 8.0, 250 mM NaCl, 2 mM DTT, and 2 mM PMSF) and lysed in a French press (Avanti cell disrupter). The cell lysate was clarified by centrifugation and loaded onto a packed column containing 5 ml of glutathione-Sepharose 4B resin (GE Healthcare). After extensive washing with lysis buffer, Ric-8At was cleaved from the resin overnight at 4 °C using a quantity of TEV protease corresponding to 10% of the total GST fusion protein estimated to be on the resin. TEV-digested protein was eluted from the GST-Sepharose 4B resin with elution buffer (50 mM Tris, pH 8.0, 2 mM DTT, and 2 mM PMSF) and dialyzed against the same buffer. The dialysate was loaded onto a UNO-Q matrix (Bio-Rad) and eluted with a 0–500 mM NaCl gradient on an AKTA FPLC system (GE Healthcare). Pure Ric-8At eluted from the matrix at 165–175 mM of NaCl. The protein was later found to be pure by SDS-PAGE analysis.

The open reading frame of rat $G\alpha_{i1}$ was amplified by PCR using attB-modified forward primer, encoding a TEV site N-terminal to the $G\alpha_{i1}$ sequence, 5′-GGGGACAGTTTGTACAAAAAAGCAGGCTACGAAAACCTATACTTTCAGGGATGTACTCTTTCTGCTGAA-, and 3′-TTTTTATTAGAATTTCTAACACCAGAAAAAACTCTGGGTCGAAAGAACATGTTTCACCAGGGG-5′ as reverse primer. The resulting PCR product was cloned into the pDEST-15 destination vector to be expressed as a GST fusion protein using the Gateway cloning system (Invitrogen). Expression and TEV digestion protocols were similar to those used for Rat Ric-8At except that $G\alpha_{i1}$ eluted at 130–140 mM of NaCl from the UNO-Q matrix. Hexahistidine-tagged $G\alpha_{i1}$ encoded in a pQE60 vector was expressed in *E. coli* strain JM-109 and purified as described earlier (44). The (W211A)$G\alpha_{i1}$ mutant was generated using the QuikChange kit according to the manufacturer's protocol

(Stratagene) using the pQE60 vector harboring wild type $G\alpha_{i1}$ as a template. After sequencing to confirm the presence of the mutation, (W211A)$G\alpha_{i1}$ was expressed and purified using the protocol developed for the wild type protein. $G\alpha_{i1}$ and the (W211A)$G\alpha_{i1}$ mutant proteins were utilized in nonmyristoylated form for all subsequent experiments.

AGS3-C, comprising residues 465–650 of rat AGS3, was cloned into the pDEST-15 destination vector as a GST fusion protein using the Gateway cloning system (Invitrogen). A tobacco etch virus protease cleavage site was inserted between coding regions for GST and AGS3-C regions. AGS3-C was purified as described earlier (40).

Yellow fluorescent protein (YFP) was appended onto the 5′ end of human M19T Ric-8A by PCR sewing and inserted into the *E. coli* expression vector, pET28a (Novagen). This construct contained the following features: 5′-His_6-NheI-YFP-EcoRI-Ric-8A-NotI-3′. His_6-YFP-Ric-8A protein was expressed in *E. coli* similarly to Ric8-At (above). The protein was purified by successive nickel-nitrilotriacetic acid (Qiagen), Hi-trap Q, and Superdex gel filtration chromatographies (GE Biosciences).

To synthesize the cyan fluorescent protein (CFP)-AGS3-C fusion protein, DNA encoding the C-terminal four GPR/GoLoco domains of rat AGS3 were amplified by PCR using the pDEST-15 vector that encoded AGS3 residues 465–650 (40). The PCR product was cloned into the NotI/XbaI sites following the CFP coding region of CFP pCDNA3.1. A 24-amino acid linker was engineered between the CFP and AGS3-C sequences. The regions encoding CFP, the linker, and residues 465–650 of AGS3 were amplified by PCR and cloned into the pDEST-15 destination vector for expression as a GST fusion protein using the Gateway cloning system (Invitrogen). A tobacco etch virus protease cleavage site was inserted between coding regions of GST and CFP. The expression vector was transformed into Bl21DE3.RIPL cells, grown in LB media containing ampicillin (120 mg/liter), and expression was induced with 500 μM isopropyl β-D-thiogalactopyranoside at 22 °C. After overnight growth, the cells were suspended in lysis buffer (50 mM Tris, pH 8.0, 300 mM NaCl, 2 mM DTT, and 5 mM PMSF), lysed by sonication, and pelleted. The clarified supernatant was loaded onto a packed column containing 5 ml of glutathione-Sepharose 4B resin (GE Healthcare) resin. After extensive washing with lysis buffer, TEV protease corresponding to 10% of the GST fusion protein was added to the resin. The reaction was allowed to proceed at 4 °C overnight. The TEV-digested protein was eluted and dialyzed against buffer (50 mM Tris, pH 8.0, 2 mM DTT, and 50 mM NaCl) to remove excess salt. The resulting CFP-AGS3-C was used for FRET assays without further purification.

AGS3-C:$G\alpha_{i1}$·GDP and AGS3-C:His_6-$G\alpha_{i1}$·GDP complexes were purified as described previously using a tandem Superdex 200/75 gel filtration matrix using an AKTA FPLC system (GE Healthcare) (40). Nucleotide-free Ric-8At:$G\alpha_{i1}$ complex was generated by incubating equimolar concentrations of Ric-8At (500 μl of 150 μM protein) with $G\alpha_{i1}$·GDP (500 μl of 150 μM protein) overnight in buffer (20 mM Tris, pH 8.0, 150 mM NaCl, 2 mM DTT, and 5 mM EDTA) containing 50 μl of immobilized alkaline phosphatase (Sigma) to hydrolyze released nucleotide, and gently rocked at 4 °C. The immobilized alkaline phosphatase was removed by centrifugation, and Ric-8At:$G\alpha_{i1}$ complex was gel-filtered over tandem Superdex 200/75 gel filtration columns pre-equilibrated in 20 mM Tris, pH 8.0, 150 mM NaCl, 2 mM DTT, and eluted at a flow rate of 0.4 ml/min using an AKTA FPLC (GE Healthcare).

[^{35}S]GTPγS Binding Assays—Binding of [^{35}S]GTPγS to $G\alpha_{i1}$ or (W211A)$G\alpha_{i1}$ was performed using a filter binding method (32). Ric-8At or YFP-Ric-8A-catalyzed [^{35}S]GTPγS binding reactions included 250 nM Ric-A8t or YFP-Ric-8A. AGS3-C or CFP-AGS3-C-inhibited binding reactions included 75 nM AGS3-C or CFP-AGS3-C. GTP binding reaction mixtures contained [^{35}S]GTPγS at a final concentration of 10 μM. Binding reactions were initiated by addition of $G\alpha_{i1}$ to a final concentration of 250 nM. Aliquots were quenched with ice-cold buffer containing 20 mM Tris-HCl, pH 7.7, 100 mM NaCl, 2 mM $MgSO_4$, 1 mM GTP, and 0.02% $C_{12}E_{10}$, applied to BA85 nitrocellulose filter, and subjected to scintillation counting. Control experiments were performed without the addition of $G\alpha_{i1}$ to quantify nonspecific binding of [^{35}S]GTPγS to Ric-8At and AGS3-C. All experiments were conducted using proteins purified from single batches of *E. coli* cells.

Competition Assays—To assay displacement of AGS3-C from the AGS3-C:His_6-$G\alpha_{i1}$·GDP complex by Ric-8At, gel-filtered AGS3-C:His_6-$G\alpha_{i1}$·GDP complex (25 μM, dissolved in 50 mM Tris, pH 8.0, 250 mM NaCl, 10 mM imidazole, 1 mM DTT, and 50 μM GDP) was incubated for 2 h at 20 °C with Ric-8At (100 μM) in a total volume of 150 μl and then allowed to bind to 50 μl of Ni^{2+} IMAC resin (Bio-Rad). The beads were washed three times with 400 μl of buffer (50 mM Tris, pH 8.0, 250 mM NaCl, 10 mM imidazole, 1 mM DTT, and 50 μM GDP), boiled in SDS-PAGE loading buffer, and run on an SDS-polyacrylamide gel. Samples of purified Ric-8At, AGS3-C, AGS3-C:His_6-$G\alpha_{i1}$·GDP, and Ric-8At:$G\alpha_{i1}$ were run as standards. Proteins were visualized by staining with Coomassie Brilliant Blue dye. To assay displacement of Ric-8At from the Ric-8At:$G\alpha_{i1}$ complex by AGS3, gel-filtered Ric-8At:$G\alpha_{i1}$ (25 μM suspended in 50 mM Tris, pH 8.0, 250 mM NaCl, 10 mM imidazole, 1 mM DTT, and 50 μM of GDP) complex was incubated for 2 h at 20 °C with AGS3-C (25 μM or 250 μM) and analyzed as described above.

Gel Filtration Assays—AGS3C:$G\alpha_{i1}$·GDP complex (14 μM complex in 20 mM Tris, pH 8.0, 250 mM NaCl, 1 mM DTT, and 10 μM of GDP) was incubated for 2 h at 20 °C with Ric-8At (100 μM) in a total volume of 1 ml and loaded on a tandem Superdex 200/75 gel filtration matrix pre-equilibrated with running buffer (50 mM Tris, pH 8.0, 150 mM NaCl, 2 mM DTT). The column was run at a constant flow rate of 0.4 ml/min, and fractions were collected. In a separate experiment, Ric-8At:$G\alpha_{i1}$ complex (100 μM, suspended in 20 mM Tris, pH 8.0, 250 mM NaCl, and 2 mM DTT) was incubated with AGS3-C (200 μM) in a total volume of 1 ml for 2 h at 20 °C and gel-filtered under the same conditions. Peak fractions of both runs were boiled with SDS-PAGE loading buffer and run on an SDS-polyacrylamide gel. The proteins were visualized by Coomassie Brilliant Blue dye.

Isothermal Titration Calorimery (ITC)—ITC experiments were performed using a VP-ITC (MicroCal) instrument. Fixed aliquots (8 μl) of $G\alpha_{i1}$·GDP (200 μM) suspended in ITC buffer (20 mM Tris, pH 8.0, 250 mM NaCl, 2 mM DTT, and 25 μM GDP)

were injected into the calorimeter cell containing 1.43 ml of AGS3-C (6 μM) in ITC buffer, and the heats at binding were recorded. Alternatively, 8-μl aliquots of AGS3-C (350 μM) in ITC buffer were injected into the calorimeter cell containing 1.43 ml of Ric-8At:$G\alpha_{i1}$ (10 μM) in ITC buffer. As a control experiment, 8-μl aliquots of $G\alpha_{i1}$·GDP (200 μM) or 8-μl aliquots of 350 μM AGS3-C, both in ITC buffer, were injected into the calorimeter cell containing 1.43 ml of ITC buffer to measure the heats of protein dilution.

Ric-8At Concentration-dependent Kinetics of $G\alpha_{i1}$ Binding to GTPγS—Kinetics of Ric-8At-assisted binding of GTPγS to $G\alpha_{i1}$ were followed by monitoring the change in intrinsic fluorescence of $G\alpha_{i1}$ at 340 nm upon exchange of GDP with GTPγS. $G\alpha_{i1}$·GDP (1 μM) in buffer composed of 20 mM HEPES, pH 8.0, 100 mM NaCl, 10 mM $MgCl_2$, 1 mM DTT, and 0.05% $C_{12}E_{10}$ in a reaction volume of 400 μl was allowed to equilibrate for 10–15 min at 30 °C in a quartz fluorescence cuvette. GTPγS (10 μM) was added to the reaction mixture in the absence or presence of Ric-8At (0.125 μM-1 μM), and the increase in fluorescence at 340 nm change was monitored upon excitation at 290 nm (45). Similar experiments were conducted using (W211A)$G\alpha_{i1}$ in the presence of 1 μM Ric-8At. Fluorescence measurements were conducted using an LS55 spectrofluorometer (PerkinElmer Life Sciences) attached to a circulating water bath to maintain a steady sample temperature. The excitation and emission slit widths were set at 2.5 nm. All exciting light was eliminated by use of a 290 nm cut-off filter positioned in front of the emission photomultiplier.

Kinetic Analysis of Ric-8At GEF Activity—Initial rates of Ric-8At-mediated $G\alpha_{i1}$ guanine nucleotide exchange were determined at different concentrations of $G\alpha_{i1}$·GDP in the presence or absence of AGS3-C. Ric-8At (50 nM) was added to buffer (20 mM HEPES, pH 8.0, 100 mM NaCl, 10 mM $MgCl_2$, 1 mM DTT, and 0.05% $C_{12}E_{10}$) containing various concentrations of $G\alpha_{i1}$·GDP (0.1–1 μM). The reactions were incubated at 30 °C for 10 min; GTPγS (10 μM) was added, and fluorescence was monitored at 340 nm upon excitation at 290 nm as described above. Initial rates were determined as a function of $G\alpha_{i1}$·GDP concentration. The same set of experiments was performed in the presence of different concentrations of AGS3-C (0.2, 0.3, and 0.4 μM). Lineweaver-Burk plots were constructed to obtain V_{max} and K_m values for Ric-8At-stimulated $G\alpha_{i1}$ GTPγS binding in the absence or presence of AGS3-C.

Stopped-flow Fluorescence Assay—A stopped-flow based assay was performed to study the formation and decay of FRET because of interaction of YFP-Ric-8A with CFP-AGS3-C:$G\alpha_{i1}$·GDP. Equal volumes of YFP-Ric-8A (50 μl of 55 μM protein) and CFP-AGS3-C:$G\alpha_{i1}$·GDP (50 μl of 12 μM protein) in stop flow buffer (20 mM HEPES, pH 8.0, 300 mM NaCl, 10 mM $MgCl_2$, 1 mM DTT, and 0.1% $C_{12}E_{10}$) were rapidly mixed into a 20-μl optical cell of a pneumatically driven stopped-flow apparatus (SFM-18MV, Applied PhotoPhysics, Leatherhead, UK). FRET emission at 527 nm upon excitation at 415 nm using a nitrogen-purged xenon arc lamp was measured for 300 s. Elimination of scattered exciting light entering the fluorescence photomultiplier was achieved using a second monochromator unit set at 527 nm. The dead time of the instrument was estimated to be 1.34 ms when used with a 20-μl cell. A control assay was performed by rapidly mixing equal volumes of YFP-Ric-8A (50 μl of 12 μM protein) with CFP-AGS3-C (50 μl of 12 μM protein) using the same experimental conditions. The basal YFP emission generated by CFP wavelength excitation light was used as the base line to quantify the FRET signal.

A stopped-flow double mixing experiment was performed to observe reassociation of YFP-Ric-8At:$G\alpha_{i1}$ with CFP-AGS3-C upon addition of GTP. The reaction mixture was composed of the products from the reaction of YFP-Ric-8A with CFP-AGS3-C:$G\alpha_{i1}$·GDP as described above. Equal volumes of YFP-Ric-8A (110 μl of 55 μM protein) and CFP-AGS3-C:$G\alpha_{i1}$·GDP (110 μl of 12 μM protein) in stop flow buffer (20 mM HEPES, pH 8.0, 300 mM NaCl, 10 mM $MgCl_2$, 1 mM DTT, and 0.1% $C_{12}E_{10}$) were rapidly mixed into an aging loop, and the FRET formation/decay reaction was allowed to proceed for 150 s. GTP (110 μl of 300 μM) in the same reaction buffer was then sequentially mixed with the aging loop product into an optical cell of the stopped-flow apparatus. FRET at 527 nm was measured for 1300 s upon excitation at 415 nm using a nitrogen-purged xenon arc lamp.

The rate of GDP release from the AGS3-C:$G\alpha_{i1}$·GDP complex was measured by rapidly mixing equal volumes of AGS3-C:$G\alpha_{i1}$·GDP (50 μl of 12 μM protein) with Ric-8At (50 μl of 55 μM protein), both suspended in release buffer composed of 20 mM HEPES, pH 8.0, 150 mM NaCl, 10 mM $MgCl_2$, 1 mM DTT, and 0.1% $C_{12}E_{10}$, and monitoring fluorescence emission at 340 nm upon excitation at 290 nm. A control experiment was performed by rapidly mixing equal volumes of AGS3-C (50 μl of 12 μM protein) with Ric-8At (50 μl of 12 μM protein), both suspended in release buffer in the absence of $G\alpha_{i1}$·GDP. To estimate the rate of GDP released by $G\alpha_{i1}$·GDP that is not in complex with AGS3-C, upon binding to Ric-8At, equal volumes of Ric-8Atand $G\alpha_{i1}$·GDP (50 μl of 55 μM protein each) in release buffer were rapidly mixed into a stopped-flow cell, and the fluorescence was monitored at 340 nm upon excitation at 290 nm. All data reported are averages of 12–15 independent experimental traces performed under identical conditions. Sequential mixing experiments were averages of 5–8 independent experimental traces performed under identical conditions. Reactions were performed at 25 °C.

RESULTS

Preliminary experiments, aimed to identify regions of Ric-8A that bind $G\alpha_{i1}$·GDP, established that residues 1–492 or 12–492 of Rat Ric-8A were sufficient to exhibit full GEF activity toward $G\alpha_{i1}$·GDP.[3] Protein expression trials indicated that, unlike the full-length rat Ric-8A (residues 1–530) that could be expressed in *Sf9* cells (32) but not at high yield in *E. coli*, the Ric-8A fragment (residues 12–492, referred to as Ric-8At; Fig. 1*A*) could be expressed in *E. coli* to produce moderate yields (5–7 mg of purified protein/liter of LB media) of protein for biophysical studies. Nonmyristoylated $G\alpha_{i1}$ was used for the studies reported here.

We found that the rate of Ric-8At-stimulated $G\alpha_{i1}$ exchange of GDP for GTPγS (0.45 min^{-1}) is comparable with that catalyzed by full-length Ric-8A purified from insect cell culture

[3] G. G. Tall and C. J. Thomas, unpublished observations.

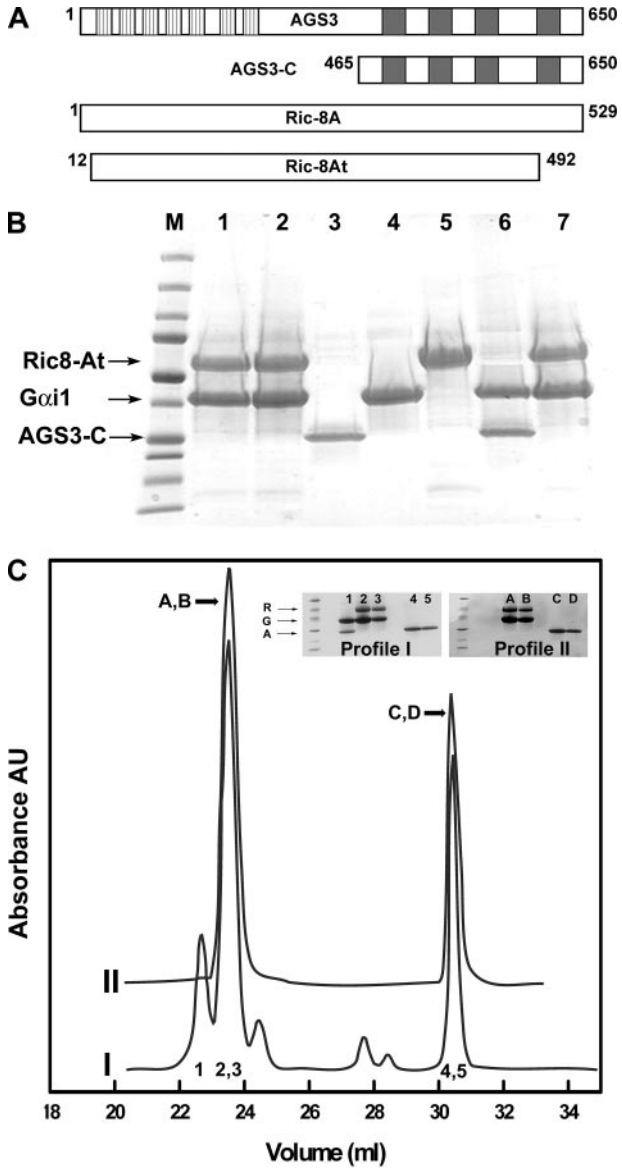

FIGURE 1. **Ric-8At induces dissociation of AGS3-C:Gα$_{i1}$·GDP, whereas AGSC-3 does not disrupt the Ric-8At:Gα$_{i1}$ complex.** *A*, schematic representation of the protein constructs used in this study. *Vertical hatched boxes* represent tetratricopeptide repeats; *gray boxes,* GPR/GoLoco repeats in AGS3. Residue numbers at N- and C-terminal boundaries of constructs are indicated. *B*, gel-filtered AGS3-C:His$_6$Gα$_{i1}$·GDP complex (25 μM) was incubated for 2 h at 20 °C with Ric-8At (100 μM) and then bound to 50 μl of Ni^{2+} IMAC resin. The resin was run on an SDS-polyacrylamide gel, and the proteins were visualized by staining with Coomassie Brilliant Blue dye (*lane 1*). Gel-filtered Ric-8At:His$_6$Gα$_{i1}$ complex (25 μM) was incubated for 2 h at 20 °C with AGS3-C (250 μM) and analyzed as above (*lane 2*). Similar results were obtained in the presence or absence of excess GDP. *Lanes 3–7* indicate the proteins AGS3 (*lane 3*), His$_6$-Gα$_{i1}$ (*lane 4*), and Ric-8 (*lane 5*) and protein complexes AGS3-C:His$_6$-Gα$_{i1}$·GDP (*lane 6*) and Ric-8At:His$_6$-Gα$_{i1}$ (*lane 7*) used in this study. *C*, AGS3-C:Gα$_{i1}$·GDP complex (14 μM) was incubated for 2 h at 20 °C with Ric-8At (100 μM) in a total volume of 1 ml, and the reaction mixture was resolved using a tandem Superdex 200/75 gel filtration matrix (*profile I*). Conversely, Ric-8At:Gα$_{i1}$ (100 μM) complex was incubated with AGS3-C (200 μM) for 2 h at 20 °C and treated under similar gel filtration conditions (*profile II*). *Inset*, the peak fractions for both experiments were analyzed by SDS-PAGE to visualize the proteins. *Insets* show Coomassie stained SDS-polyacrylamide gels corresponding to peaks from profiles I and II. Peaks and corresponding lanes for profile I are labeled *1–5* and for profile II labeled *A–D*.

(0.35 min^{-1}). This amounts approximately to a 12-fold increase over the intrinsic nucleotide exchange rate of Gα$_{i1}$ (32). Ric-8At, like full-length Ric-8A, binds to Gα$_{i1}$·GDP and, upon release of GDP, forms a stable, gel-filterable nucleotide-free complex. Upon addition of GTPγS, the complex dissociates rapidly to form free Ric-8At and GTPγS-bound Gα$_{i1}$ (data not shown).

The C-terminal fragment of AGS3 (residues 465–650), consisting of four GPR/GoLoco motifs (*AGS3-C*; Fig. 1*A*), functions as a GDI toward Gα$_{i1}$·GDP and forms a stable gel-filterable AGS3-C:Gα$_{i1}$·GDP complex (39, 40). To determine whether Ric-8A can induce dissociation of Gα$_{i1}$·GDP from AGS3-C, we incubated Ric-8At with a gel-filtered complex of AGS3-C with His$_6$-tagged Gα$_{i1}$·GDP for 2 h at 20 °C. The reaction mixture was then resolved by Ni^{2+} IMAC. SDS-PAGE analysis of the IMAC eluant showed that Ric-8At displaced AGS3-C from the AGS3-C:His$_6$-Gα$_{i1}$·GDP complex to form a Ric-8At:Gα$_{i1}$ complex (Fig. 1*B*, *lane 1*). To test whether the converse is true, that AGS3-C causes dissociation of Gα$_{i1}$ from Ric-8At, we incubated AGS3-C with Ric-8At:His$_6$-Gα$_{i1}$ complex and treated the mixture as described above. Intact Ric-8At:His$_6$-Gα$_{i1}$ complex was retained on the Ni^{2+}-IMAC column showing that nucleotide-free Ric-8At:His$_6$-Gα$_{i1}$ complex does not dissociate in the presence of AGS3-C, even at 50-fold molar excess to Ric-8At (Fig. 1*B*, *lane 2*). Gel filtration chromatography of mixtures, containing either AGS3-C:Gα$_{i1}$·GDP and Ric-8At or Ric8-At:Gα$_{i1}$ and AGS3-C, showed that Ric-8At can displace Gα$_{i1}$ from the complex with AGS3-C. AGS3-C, on the other hand, does not form a stable complex with Gα$_{i1}$ bound to Ric-8At:Gα$_{i1}$ (Fig. 1*C*).

Isothermal titration calorimetry (ITC) was performed to rule out the possibility of weak interactions between AGS3-C and Ric8-At:Gα$_{i1}$. ITC measurements showed that binding of Gα$_{i1}$·GDP to AGS3-C is exothermic and indicated that four molecules of Gα$_{i1}$·GDP bind to one molecule of AGS3-C, in agreement with previously published results (40) (Fig. 2). In contrast, isothermal titration of AGS3-C into a solution containing Ric8-At:Gα$_{i1}$ complex generated no significant heat of formation (Fig. 2).

Binding of GTPγS to wild type Gα$_{i1}$ is accompanied by an increase in tryptophan fluorescence at 340 nm (45). The change in fluorescence upon addition of GTPγS binding to Gα$_{i1}$ in the presence of equimolar amounts of Ric-8At is 10–12-fold faster than that observed in the absence of Ric-8At (Fig. 3). This rate enhancement is consistent with data published earlier using radioactive [^{35}S]GTPγS filter binding assays to monitor Ric-8A-assisted GTPγS uptake by Gα$_{i1}$ (32). This increase in fluorescence is because of structural changes at the nucleotide-binding site of Gα$_{i1}$, because no fluorescence enhancement was observed for Ric-8At-catalyzed GTPγS binding for (W211A)Gα$_{i1}$ in which Trp-211 was replaced by alanine (Fig. 3*A*, *blue trace*). However, filter binding experiments using radiolabeled [^{35}S]GTPγS showed that Ric-8At catalyzes GTPγS binding to (W211A)Gα$_{i1}$ at a rate similar to that for wild type Gα$_{i1}$ (supplemental Fig. 1). The rate of [^{35}S]GTPγS binding to (W211A)Gα$_{i1}$ determined by this method is 0.031 min^{-1}, and the Ric-8At-stimulated rate is 0.38 min^{-1}. In comparison, the rate of [^{35}S]GTPγS binding to wild type Gα$_{i1}$ is 0.038 min^{-1}, and the Ric-8At-assisted rate is 0.43 min^{-1}. Experiments conducted in the presence of varying concentrations of Ric-8At showed that the fluorescence-based method

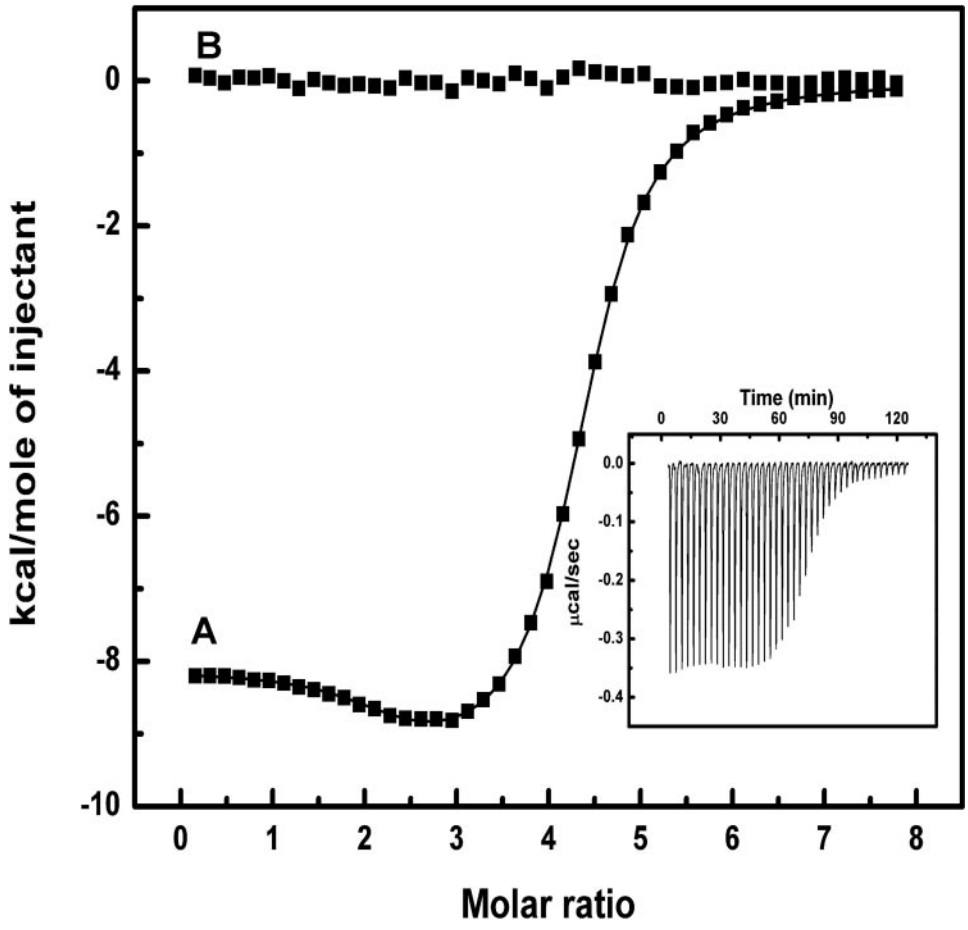

FIGURE 2. **Isothermal titration calorimetric analysis of the interactions of AGS3-C with Gα$_{i1}$·GDP and AGS3-C with Ric-8At:Gα$_{i1}$.** Fixed aliquots (8 μl) of Gα$_{i1}$·GDP (200 μM) were injected into a calorimetric cell containing 1.43 ml of AGS3-C (6 μM), and the heat released was recorded (*trace A*, thermogram shown in *inset*). Data were fit by nonlinear least squares to a "two independent sets of sites" model, showing that four molecules of Gα$_{i1}$·GDP bind to one molecule of AGS3-C and that binding is cooperative. Shown in *trace B*, fixed aliquots (8 μl) of AGS3-C (350 μM) were injected into 1.43 ml of Ric-8At:Gαil (10 μM) complex. No significant heats were generated in course of this reaction.

can be used to quantify the catalytic activity of Ric-8At as a GEF toward Gα$_{i1}$ subunits (Fig. 3). We assayed the rate of exchange of GDP for GTPγS at various concentrations of Gα$_{i1}$·GDP in the presence of a fixed concentration of Ric-8At. Lineweaver-Burk analysis of these rate profiles yielded a V_{max} of 0.37 μM min^{-1} and a K_m of 1 μM for the binding of GTPγS to Gα$_{i1}$ in the presence of Ric-8At (Fig. 4).

The observation that Ric-8At is able to displace AGS3-C from an AGS3-C:Gα$_{i1}$·GDP complex suggests that AGS3-C, as a GDI, may function as an inhibitor of Ric-8At-catalyzed Gα$_{i1}$ guanine nucleotide exchange activity. Earlier studies demonstrated that high concentrations of AGS3-C and the paralogous protein LGN-C indeed act as inhibitors of Ric-8A GEF activity (42). To test the activity of AGS3-C as an inhibitor of Ric-8At GEF action, and to determine the kinetic mechanism of inhibition, we assayed the rate of Ric-8At-catalyzed exchange of GDP for GTPγS at different concentrations of AGS3-C. In the presence of AGS3-C, the V_{max} for Ric-8At-catalyzed nucleotide exchange was reduced, but the K_m value was not affected significantly (Fig. 4). Therefore, AGS3-C acts as a noncompetitive inhibitor of Ric-8At, suggesting that AGS3-C and Ric-8At may bind to different sites on Gα$_{i1}$·GDP.

The noncompetitive mode by which AGS3-C inhibits Ric-8At permits the speculation that Ric-8At might bind to the AGS3-C:Gαil·GDP complex and form a transient multimeric Ric-8At:AGS3-C:Gα$_{i1}$ complex. To test this hypothesis, we reasoned that the association between an N-terminally YFP-tagged Ric-8At and a complex of Gα$_{i1}$·GDP with CFP-tagged AGS3-C would result in production of a transient FRET signal upon irradiation at the fluorescence excitation wavelength of CFP. CFP- and YFP-tagged proteins were expressed in *E. coli*, purified to near-homogeneity, and used in subsequent binding assays. By the use of gel filtration and [^{35}S]GTPγS binding and fluorescence assays, we determined that YFP-Ric-8A and CFP-AGS3-C exhibit GEF and GDI activities, respectively, toward Gαil·GDP (supplemental Fig. 2).

A rapid mixing experiment was designed to monitor the interaction of YFP-Ric-8A with CFP-AGS3-C:Gα$_{i1}$·GDP. Equal volumes of these two proteins in identical buffers were rapidly mixed in the cell of a pneumatically driven stopped-flow apparatus, and the evolution of FRET at 527 nm upon excitation of CFP at 415 nm was measured. The evolution of FRET after mixing exhibited two distinct phases. The initial phase, an additive value of the FRET and basal YFP fluorescence lasting ~15–20 s, consisted of a sharp rise in fluorescence to a maximal value, which was followed by a second phase characterized by a monotonic decay in fluorescence back to the basal (415 nm wavelength excited) YFP levels (Fig. 5, *top panel*, *green trace*). The magnitude and rate of the initial portion of the FRET signal were found to be dependent on the concentration of the two reacting species. Analysis of the evolution of FRET intensity over a range of YFP-Ric-8A and CFP-AGS3-C concentrations yielded a second-order association constant for the two species of 6.3×10^3 min^{-1} M^{-1}. The monotonic decay phase was concentration-independent and proceeded at a rate of 1.2 min^{-1}. We attribute this phase to dissociation of the YFP-Ric-8A:CFP-AGS3-C·Gα$_{i1}$ complex following the release of AGS3 and GDP from Gα$_{i1}$. A control experiment wherein equal volumes of YFP-Ric-8A and CFP-AGS3-C were rapidly mixed under identical conditions produced no fluorescence fluctuations at the YFP emission wavelength, corresponding only to the basal YFP (415 nm wavelength excited) fluorescence (Fig. 5, *top panel*, *black trace*). Similarly, the rapid mixing of YFP-Ric-8A·Gα$_{i1}$ complex with CFP-AGS3-C produced no significant fluores-

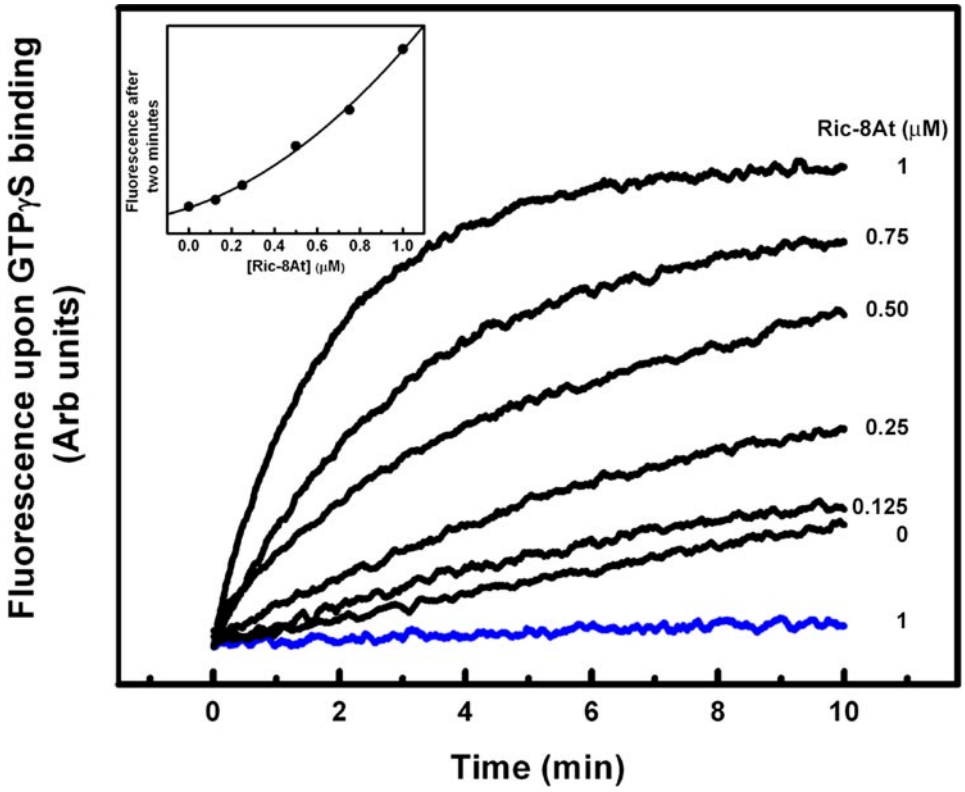

FIGURE 3. **Ric-8At catalyzes GTPγS binding to Gα$_{i1}$.** Kinetics of Ric-8At-assisted binding of GTPγS to Gα$_{i1}$ was followed by tryptophan fluorescence. 400 μl of Gα$_{i1}$·GDP (1 μM) was equilibrated for 10–15 min at 25 °C in a fluorescence cuvette. 10-Fold excess of GTPγS was added to Gα$_{i1}$, and fluorescence at 340 nm upon excitation at 290 nm was monitored in the absence or presence of Ric-8At (1, 0.75, 0.5, 0.25, 0.125, and 0 μM; *black traces* from *top to bottom*). A similar experiment under the same conditions and in the presence of 1 μM Ric-8A was conducted with the W211A mutant of Gα$_{i1}$ (*blue trace*). *Inset,* tryptophan fluorescence at the 2-min time points of the reaction as a function of increasing Ric-8At concentration.

cence changes at the YFP emission wavelength (data not shown).

We then sought to determine whether the nucleotide-free YFP-Ric-8At:Gα$_{i1}$ complex formed after the reaction of YFP-Ric-8At with CFP-AGS3-C:Gα$_{i1}$·GDP is capable of cycling through a round of GTP binding, with the release of Ric-8At, and hydrolysis. This, in turn, would allow reformation of the AGS3:Gα$_{i1}$·GDP complex and transient association with Ric-8At as described above. A sequential mixing experiment was designed such that a mixture of YFP-Ric-8At with CFP-AGS3-C:Gα$_{i1}$·GDP was aged in a delay loop for 150 s to ensure formation of YFP-Ric-8At:Gα$_{i1}$, free AGS3-C, and GDP as shown in the *green trace* in Fig. 5, *bottom panel*. This reaction is the same as that illustrated in Fig. 5, *top panel*. The contents of the delay loop were then rapidly mixed with excess GTP in the optical cell of the stopped-flow apparatus. This resulted in a slow rise in FRET intensity lasting ~450 s. This FRET signal then returns to basal values in ~700 s (*black trace* in Fig. 5, *bottom panel*). We attribute the rise and fall of FRET intensity shown in this latter phase to these following five steps: 1) rapid formation of Gα$_{i1}$·GTP and free YFP-Ri8At upon addition of GTP to YFP-Ric-8At:Gα$_{i1}$; 2) hydrolysis of GTP to yield Gα$_{i1}$·GDP; 3) association of Gα$_{i1}$·GDP with CFP-AGS3-C or with YFP-Ric-8At (the latter would lead to recycling through step 1); 4) association of free YFP-Ric-8At with the CFP-AGS3-C:Gα$_{i1}$·GDP complex, accompanied by induction of FRET; and 5) dissociation of the ternary complex accompanied by YFP-Ric-8At-catalyzed release of GDP from Gα$_{i1}$ and formation of YFP-Ric-8A·Gα$_{i1}$ complex. This is concomitant with dissociation of CFP-AGS3-C from Gα$_{i1}$ and from YFP-Ric-8A, with consequent decay of FRET emission. Because GTP is present in excess, several rounds of this series of reactions can occur, accounting for the gradual decay of FRET over the course of several minutes. This cycle of reactions is depicted schematically in Fig. 6.

To elucidate the kinetic relationship between dissociation of the AGS3-C from Ric-8At:AGS3-C:Gα$_{i1}$·GDP and dissociation of GDP from Gα$_{i1}$ mediated by Ric-8At, we conducted rapid mixing experiments similar to those described above, but we monitored the release of GDP from Gα$_{i1}$ as a function of Trp-211 fluorescence loss. Earlier experiments indicated that binding of AGS3-C to Gα$_{i1}$·GDP does not induce a change in fluorescence at 340 nm (data not shown), because AGS3-C stabilizes the GDP-bound, low fluorescence state of Gα$_{i1}$, and AGS3-C itself lacks tryptophan residues. We also established that, upon formation of a nucleotide-free complex with Ric-8At, there is a decrease in the intrinsic fluorescence of Gα$_{i1}$ because of Trp-211 (this effect is not observed upon complexation with (W211A)Gα$_{i1}$). By utilizing this effect, we monitored the rate of GDP release from a preformed complex of AGS3-C:Gα$_{i1}$·GDP upon addition of stoichiometric amounts of Ric-8At, and we found that it proceeded at a rate of 0.38 min^{-1} (Fig. 5, *top panel, red trace*). Addition of a 5-fold molar excess of Ric-8At to the complex increased the rate of fluorescence quenching to 0.49 min^{-1} (Fig. 5, *top panel, blue trace*). The processes subsumed in these rates include association of Ric-8At with AGS3-C:Gα$_{i1}$·GDP and possibly dissociation of AGS3 from the transient complex with Ric-8At and Gα$_{i1}$ as well as GDP dissociation from the latter.

DISCUSSION

Recent biochemical studies demonstrated that Ric-8A, a mammalian GEF for G$_i$ and G$_q$ class G-protein α subunits, is able to catalyze exchange of GTP for GDP from Gα$_{i1}$·GDP bound to LGN or the LGN:NuMA complex (42). LGN, like its paralog AGS3, contains four GPR/GoLoco repeats, each of which binds exclusively to a GDP-bound Gα subunit and inhibits its nucleotide release (34, 46). LGN also weakly inhibits the GEF activity of Ric-8A toward Gα$_{i1}$·GDP (42). Experiments conducted in our laboratory showed that AGS3-C can also inhibit Ric-8A GEF activity. These observations prompted us to ask

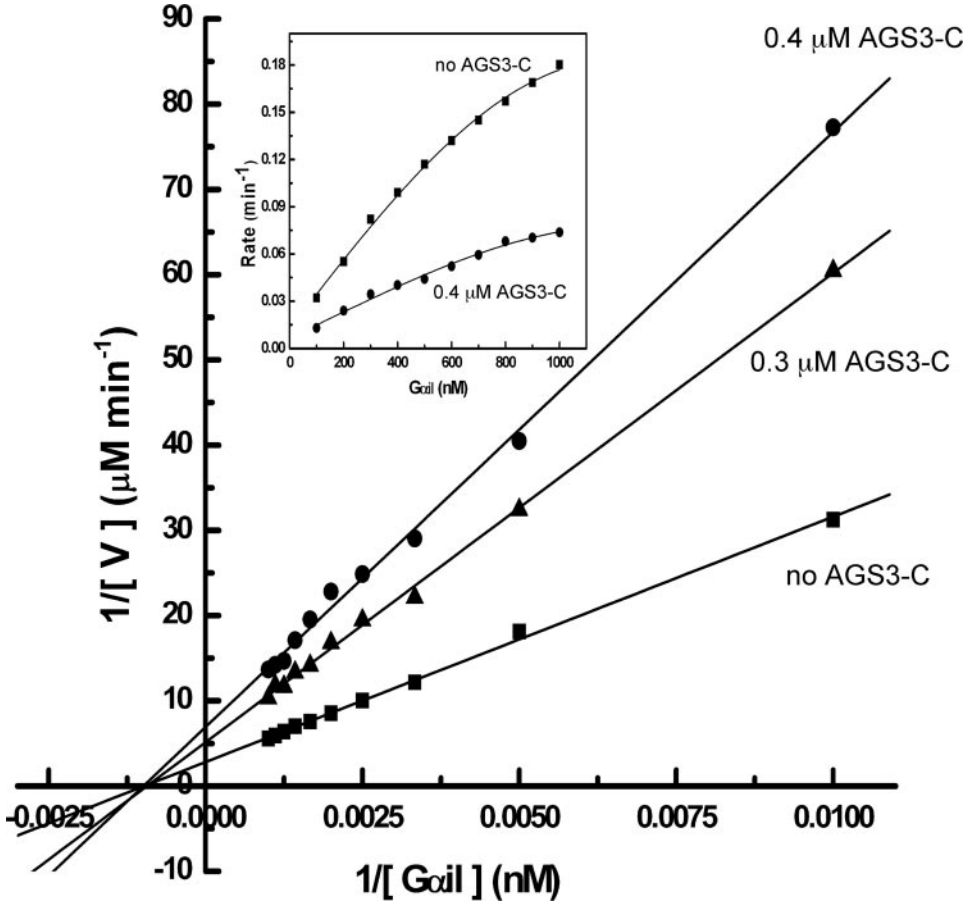

FIGURE 4. **AGS3-C is a noncompetitive inhibitor of Ric-8At-catalyzed exchange of GDP by GTPγS on Gα$_{i1}$.** Lineweaver-Burk plot of the initial velocities of Ric-8At-catalyzed guanine nucleotide exchange determined as a function of substrate (Gα$_{i1}$·GDP) concentration (*Inset*). Reaction mixtures contained Ric-8At (50 nM), Gα$_{i1}$ (0.1–1 μM) and 10 μM GTPγS. Nucleotide binding was monitored by tryptophan fluorescence as indicated in Fig. 3. Experiments were conducted in the absence of AGS3-C (■), 0.3 μM (▲), or 0.4 μM (●) AGS3-C.

whether Ric-8A competes directly with AGS3-C in binding to Gα$_{i1}$·GDP or, as suggested by Tall *et al.* (42), is able to bind directly to the AGS3:Gα$_{i1}$·GDP complex.

The experiments described here illustrate a key point regarding the physiological function of Ric-8A action upon AGS3:Gα$_{i1}$·GDP. The effects of Ric-8A cannot be reversed by AGS3 or LGN within the same round of the G-protein catalytic cycle. Protein pulldown and gel filtration experiments show that the AGS3-C:Gα$_{i1}$·GDP complex dissociates in the presence of Ric-8At, whereas the Ric-8At:Gα$_{i1}$ complex does not dissociate in the presence of AGS3-C. Gel filtration experiments confirm the pulldown assay results and further indicate that incubation of Ric-8At with AGS3-C:Gα$_{i1}$·GDP yields GDP and nucleotide-free Ric-8At:Gα$_{i1}$ complex. The high affinity of Ric-8At for nucleotide-free Gα$_{i1}$ and the low affinity of AGS3-C toward the same are probably the underlying causes of this irreversibility. The difficulty in isolating active Gα$_{i1}$ in the nucleotide-free state prohibits direct testing of this hypothesis. However, the absence of heat evolution or absorption upon isothermal titration of Ric-8At:Gα$_{i1}$ with AGS3-C strongly suggests that AGS3-C does not bind to nucleotide-free Ric-8A·Gα$_{i1}$ near physiological temperatures.

Ric-8A acts catalytically to promote the exchange of GDP for GTP (or that of GTP analogs) upon its substrate, Gα$_{i1}$·GDP (32). We have used nonmyristoylated Gα$_{i1}$ for experiments described here. The rate of Ric-8A-stimulated nucleotide exchange is reported to be 2-fold greater for myristoylated *versus* unmodified Gα$_{i1}$, and the reaction is less sensitive to inhibition by GPR/GoLoco proteins (42). Thus, quantitative but not qualitative differences from the results reported here would be expected for similar experiments conducted with myristoylated Gα$_{i1}$.

The Ric-8At:Gα$_{i1}$ complex is a stable and readily isolatable intermediate of this reaction that dissociates rapidly in the presence of GTP to yield Ric-8At and Gα$_{i1}$·GTP. The data presented here show that Ric-8At catalyzes GTPγS binding to Gα$_{i1}$ with a K_m for Gα$_{i1}$·GDP of ~1 μM and a turnover number (k_{cat}) near 8 min^{-1}. AGS3-C is a noncompetitive inhibitor of Ric-8At and reduces V_{max}, but it does not affect the K_m value for Gα$_{i1}$·GDP. The K_i value for AGS3-C appears to be less than 1 μM, but it was not accurately determined in our experiments. That AGS3-C is a noncompetitive inhibitor of Ric-8A with respect to Gα$_{i1}$ suggests the possibility that Ric-8A and AGS3 bind to distinct sites on Gα$_{i1}$.

We have conducted time-resolved FRET experiments that conclusively demonstrate that CFP-AGS3-C:Gα$_{i1}$·GDP interacts with YFP-Ric-8A to form a ternary complex with a second-order rate constant of 6.3×10^3 min^{-1} M^{-1}. The FRET signal subsequently decays (at the rate of 1.2 min^{-1}) back to the basal YFP fluorescence levels. The strong transient FRET emission seen in our experiments indicates that at least one YFP domain is present within a Förster radius <50 Å of the CFP tag of AGS3-C. Because Ric-8At does not bind to AGS3-C, FRET can arise only from binding of YFP-Ric-8A to Gα$_{i1}$·GDP present in a CFP-AGS3-C:Gα$_{i1}$·GDP complex. Control experiments rule out the possibility that FRET arises from nonspecific interactions between YFP-Ric-8A and CFP-AGS3-C.

We note that it was not possible to determine the stoichiometry of the transient ternary complex composed of Gα$_{i1}$·GDP, AGS3-C, and Ric-8At. At the protein concentrations used in these experiments, three to four molecules of Gα$_{i1}$ may be expected to bind to the four available GPR/GoLoco motifs in N-terminally CFP-tagged AGS3-C. However, the magnitude of FRET emission that arises from binding of YFP-Ric-8A to each of the four possible Gα$_{i1}$ molecules arrayed on CFP-AGS3-C may differ, and the four Gα$_{i1}$ molecules may not be equally accessible for interaction with YFP-Ric-8A. Binding of even a single YFP-Ric-8A molecule to one of four interaction sites in

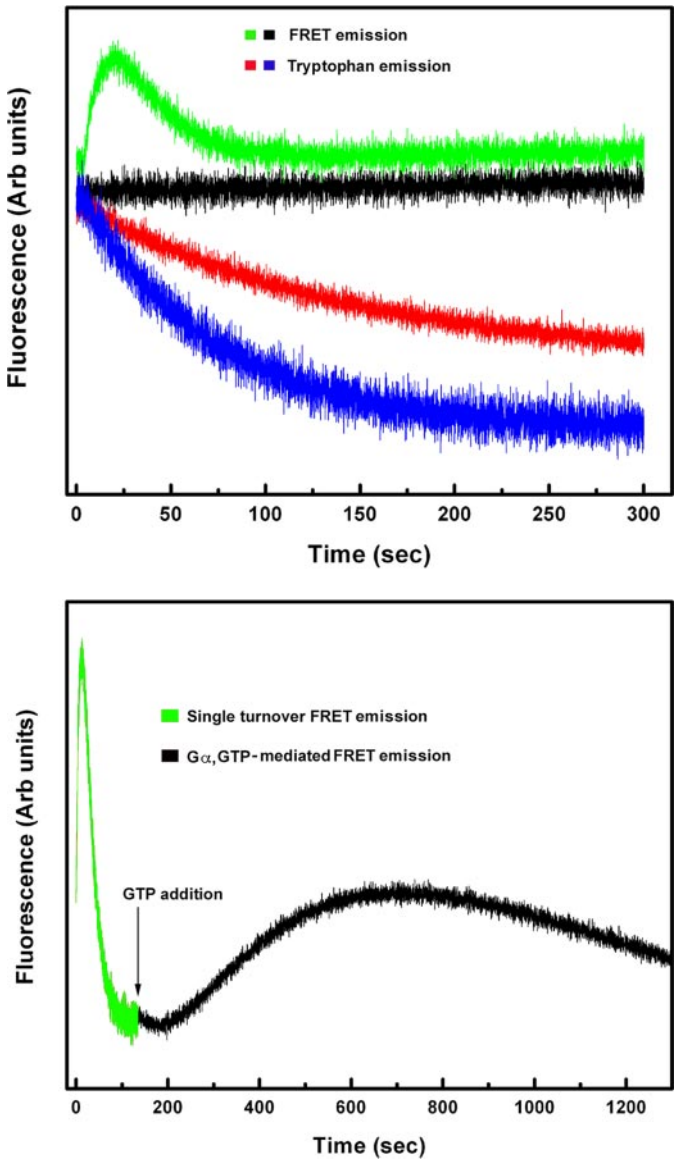

FIGURE 5. **FRET detection of transient ternary complex formation by YFP-Ric-8A with CFP-AGS3-C:$G\alpha_{i1}$·GDP.** *Top panel*, evolution and decay of FRET emission resulting from the interaction of YFP-Ric-8A with CFP-AGS3-C:$G\alpha_{i1}$·GDP. 120 μl of YFP-Ric-8A (55 μM) was mixed rapidly with an equal volume of CFP-AGS3:$G\alpha_{i1}$·GDP (12 μM) in a 20-μl cell of a pneumatically driven stopped-flow apparatus. FRET emission fluorescence at 527 nm upon excitation at 415 nm was measured for 300 s (*green trace*). A control experiment was performed by rapidly mixing equal volumes (120 μl) of YFP-Ric-8A (55 μM) with CFP-AGS3-C (12 μM) under the same reaction conditions (*black trace*). Traces shown are averages of 12–15 independent experiments performed under identical conditions. GDP release from AGS3-C:$G\alpha_{i1}$·GDP (50 μl, 12 μM) was monitored by tryptophan fluorescence emission (340 nm) after rapid mixing with 50 μl of Ric-8At (55 μM, *red trace*, or 250 μM, *blue trace*). *Bottom panel*, evolution of FRET because of addition of GTP to a reaction mixture identical to that shown in the *top panel* at the 150-s time point. Equal volumes of YFP-Ric-8A (110 μl, 55 μM) and CFP-AGS3-C:$G\alpha_{i1}$·GDP (12 μM complex) were rapidly mixed into an aging loop. After 150 s, GTP (110 μl, 150 μM) was then mixed with 110 μl of the aging loop contents into the optical cell of the stopped-flow apparatus (note that, because of the 1:4 stoichiometry of the CFP-AGS3-C:$G\alpha_{i1}$·GDP complex, the concentration of GTP injected into the optical cell is in ~3-fold excess to $G\alpha_{i1}$). FRET emission at 527 nm was measured for 1300 s. The *green trace* represents the reaction sequence depicted in *top panel*, and the *black trace* shows the evolution of FRET emission because of association of CFP-AGS3-C:$G\alpha_{i1}$·GDP with YFP-Ric-8A upon GTP binding and hydrolysis by $G\alpha_{i1}$. *Arrow* indicates the time point at which GTP was added to the aged reaction mixture. The FRET emission base line for first reaction sequence at 150 s (*green trace*) was aligned with that for the second phase of the reaction (*black trace*).

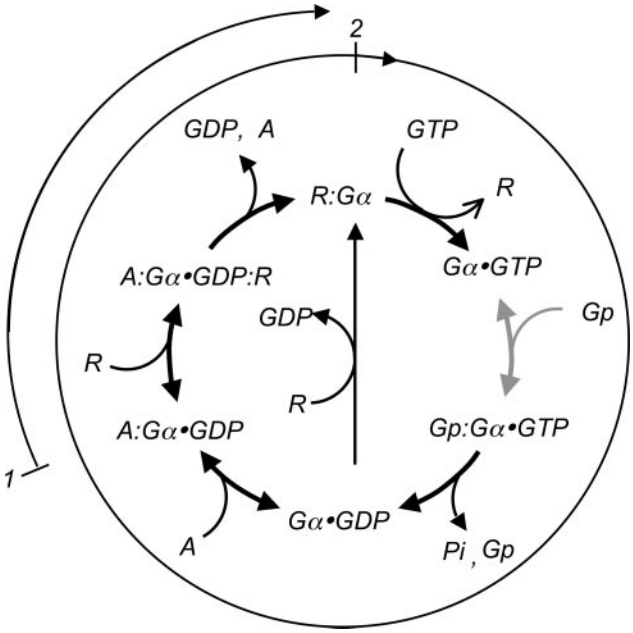

FIGURE 6. **A cycle of nonreceptor-mediated guanine nucleotide binding and hydrolysis by $G\alpha_{i1}$.** The cycle includes $G\alpha_{i1}$ (*Gα*), in the presence of Ric-8A (*R*), AGS3-C (*A*), and a hypothetical GAP protein (*Gp*) (reactions involving the latter are shown in *gray*, because GAP proteins were not included in the present work). Kinetically reversible reactions are shown with *double-headed arrows*. The *outer arc* (labeled *1*) describes the reaction, initiated at the point indicated by the *perpendicular bar*, corresponding to the *green FRET traces* shown in Fig. 5. The *inner circle* (labeled *2*) describes the cyclic course of the reaction initiated at the point indicated by the perpendicular bar, corresponding to the *black FRET trace* in Fig. 5, *bottom panel*.

CFP-AGS3-C:$G\alpha_{i1}$·GDP could potentially generate FRET emission. Likewise, subsequent decay of FRET emission to the basal state could be due largely to dissociation of a single YFP-Ric-8A from the CFP-AGS3-C complex.

Dissociation (or loss of FRET from) of the YFP-Ric-8A:CFP-AGS3-C complex must arise through a spontaneous change in state of the complex subsequent to its formation. Ric-8At-catalyzed release of GDP from one or more $G\alpha_{i1}$ molecules bound to CFP-AGS3-C might induce such a change. Formation of nucleotide-free Ric-8At:$G\alpha_{i1}$ is associated with quenching of $G\alpha_{i1}$ tryptophan fluorescence (Fig. 5, *red* and *blue traces*). Quenching upon addition of Ric-8At to the AGS-3C:$G\alpha_{i1}$·GDP complex occurs with a rate constant (0.38 min^{-1}) that is only slightly slower than the quenching rate when Ric-8At binds to and releases nucleotide from free $G\alpha_{i1}$·GDP (~0.50 min^{-1}). Hence, disassembly of the $G\alpha_{i1}$:AGS3-C by Ric-8At apparently occurs two to three times more rapidly than the rate at which Ric-8A stimulates dissociation of GDP from $G\alpha_{i1}$, as illustrated by Scheme 1 (in which unitary stoichiometry among components is assumed for simplicity).

$$\text{AGS3:G}\alpha\text{·GDP} + \text{Ric8A} \leftrightarrow \text{AGS3:G}\alpha\text{·GDP:Ric8A} \rightarrow$$

$$\text{AGS3} + \text{Ric8A:G}\alpha\text{·GDP} \rightarrow \text{Ric8A:G}\alpha + \text{GDP}$$

SCHEME 1

Either of two mechanisms would be consistent with the observed kinetics of FRET emission and GDP release described above. In one scheme, the YFP-Ric8-At:$G\alpha_{i1}$·GDP:CFP-AGS3-C complex undergoes a spontaneous rearrangement

that results in the release of AGS3-C from the complex and subsequent dissociation of GDP from Ric-8At:$G\alpha_{i1}$·GDP. Alternatively, dissociation of $G\alpha_{i1}$ molecules from the four AGS3-C GPR/GoLoco motifs could occur cooperatively, triggered by Ric-8At-catalyzed GDP release from one or two $G\alpha_{i1}$ molecules in the complex. Support for the latter model comes from the observation that assembly of AGS3-C:$G\alpha_{i1}$·GDP complexes may be cooperative (40).

Our sequential mixing experiments indicate that the nucleotide-free $G\alpha_{i1}$ in YFP-Ric-8At:$G\alpha_{i1}$ complex is competent to undergo additional nucleotide binding/hydrolysis cycling reactions when liberated by Ric-8At from an initial AGS3-C-bound state as shown schematically in Fig. 6. This cycling process is akin to the classical receptor-mediated G-protein cycling event, but it should be stressed that, unlike the receptor that recognizes only the G-protein heterotrimers, Ric-8A can bind to both free $G\alpha_{i1}$·GDP and AGS3-bound $G\alpha_{i1}$·GDP.

The results presented here have implications for the molecular mechanism of Ric-8A action. That Ric-8A and AGS3-C are capable of forming a transient complex with $G\alpha_{i1}$ implies that the two must occupy distinct or at least partially nonoverlapping binding sites. The crystal structure of the GPR/GoLoco peptide of RGS14 bound to $G\alpha_{i1}$·GDP revealed interactions between the peptide and the Switch I and Switch II segments of $G\alpha_{i1}$ extending across the catalytic site and into the helical domain (41). Because Ric-8A and AGS3-C form a transient complex with $G\alpha_{i1}$, Ric-8A is likely to interact with at least one site that lies outside of this region. Because the K_m value of Ric-8A for $G\alpha_{i1}$ is not affected by AGS3-C, it is probable that the binding sites for the two proteins on $G\alpha_{i1}$ do not overlap. The $G\alpha$-binding site for G-protein-coupled receptors, which also catalyze release of GDP from G-proteins, include C-terminal residues of $G\alpha$ that are distinct from the switch regions (47–49). GPCRs interact most productively with G-protein $\alpha\beta\gamma$ heterotrimers. AGS3 and $G\beta\gamma$ both bind to the switch segments of the GDP-bound form of $G\alpha$ to inhibit nucleotide release (6, 41). It is reasonable to propose that the $G\alpha$-binding sites for Ric-8A and GPCRs are the same or share similar structural elements.

Ric-8A is a GEF capable of acting on either free and or GPR/GoLoco-bound $G\alpha$il·GDP subunits (32). Because Ric-8A is a cell matrix or peri-centriolar protein that cannot catalyze nucleotide exchange of $G\beta\gamma$-bound $G\alpha_{il}$ (32), it does not compete directly with receptor-mediated signaling. Ric-8A may serve as the upstream regulator of $G\alpha_{i1}$ subunits in a pathway that directs dynamic aster-microtubule events during cell division. In this pathway, Ric-8A may activate receptor-independent $G\alpha_{il}$ catalysis by catalyzing GDP → GTP exchange. Catalysis would be completed by the concerted action of GAP proteins, such as *C. elegans* RGS7 that deactivate $G\alpha_i$ through acceleration of GTP hydrolysis (Fig. 6) (27). In this context, $G\alpha_i$ activation and deactivation may be coupled, respectively, to the release and sequestration of the microtubule-binding protein NuMA from the AGS3 homolog LGN. When bound to $G\alpha_i$·GDP, LGN recruits NuMA to the cell periphery while preventing its association with microtubules (43). Ric-8A has been shown, *in vitro*, to liberate NuMA from LGN through control of allosteric $G\alpha_i$·GDP binding. Liberated NuMA potentially participates in interactions with microtubules. We have speculated that this functional cycle might be responsible for generation of the pulsatile aster microtubule pulling forces that act upon the mitotic spindle. That Ric-8A is able to act on $G\alpha$il·GDP subunits that are cooperatively assembled on LGN or AGS3 suggests that Ric-8A-assisted G-protein cycling evolved primarily for multiple and rapid activation events. The unidirectional nature of the reaction is ensured by the fact that AGS3 cannot interact with Ric-8A:$G\alpha_{i1}$ complex following GDP release, or with $G\alpha$·GTP that is generated subsequently.

Acknowledgments—We are grateful to Bryant G. Oliverson and Anand Srinivasan for excellent technical support and to Alfred G. Gilman for support of this project.

REFERENCES

1. Gilman, A. G. (1987) *Annu. Rev. Biochem.* **56,** 615–649
2. Rasmussen, S. G., Choi, H. J., Rosenbaum, D. M., Kobilka, T. S., Thian, F. S., Edwards, P. C., Burghammer, M., Ratnala, V. R., Sanishvili, R., Fischetti, R. F., Schertler, G. F., Weis, W. I., and Kobilka, B. K. (2007) *Nature* **450,** 383–387
3. Cherezov, V., Rosenbaum, D. M., Hanson, M. A., Rasmussen, S. G., Thian, F. S., Kobilka, T. S., Choi, H. J., Kuhn, P., Weis, W. I., Kobilka, B. K., and Stevens, R. C. (2007) *Science* **5854,** 1258–1265
4. Mixon, M. B., Lee, E., Coleman, D. E., Berghuis, A. M., Gilman, A. G., and Sprang, S. R. (1995) *Science* **270,** 954–960
5. Coleman, D. E., Berghuis, A. M., Lee, E., Linder, M. E., Gilman, A. G., and Sprang, S. R. (1994) *Science* **265,** 1405–1412
6. Wall, M. A., Coleman, D. E., Lee, E., Iniguez-Lluhi, J. A., Posner, B. A., Gilman, A. G., and Sprang, S. R. (1995) *Cell* **83,** 1047–1058
7. Watson, N., Linder, M. E., Druey, K. M., Kehrl, J. H., and Blumer, K. J. (1996) *Nature* **383,** 172–175
8. Tesmer, J. J., Berman, D. M., Gilman, A. G., and Sprang, S. R. (1997) *Cell* **89,** 251–261
9. Blumer, J. B., Smrcka, A. V., and Lanier, S. M. (2007) *Pharmacol. Ther.* **113,** 488–506
10. Hampoelz, B., and Knoblich, J. A. (2004) *Cell* **119,** 453–456
11. Manning, D. R. (2003) *Sci. STKE 2003,* PE35
12. Goulding, M. B., Canman, J. C., Senning, E. N., Marcus, A. H., and Bowerman, B. (2007) *J. Cell Biol.* **178,** 1177–1191
13. Horvitz, H. R., and Herskowitz, I. (1992) *Cell* **68,** 237–255
14. Cho, H., and Kehrl, J. H. (2007) *J. Cell. Biol.* **178,** 245–255
15. Cho, H., and Kehrl, J. H. (2008) *Cell Cycle* **7,** 573–577
16. Wilkie, T. M., and Kinch, L. (2005) *Curr. Biol.* **15,** R843–R854
17. Reynolds, N. K., Schade, M. A., and Miller, K. G. (2005) *Genetics* **169,** 651–670
18. Blumer, J. B., Lord, K., Saunders, T. L., Pacchioni, A., Black, C., Lazartigues, E., Varner, K. J., Gettys, T. W., and Lanier, S. M. (2008) *Endocrinology*, in press
19. Bringmann, H., Cowan, C. R., Kong, J., and Hyman, A. A. (2007) *Curr. Biol.* **17,** 185–191
20. Bergmann, D. C., Lee, M., Robertson, B., Tsou, M. F., Rose, L. S., and Wood, W. B. (2003) *Development* (*Camb.*) **130,** 5731–5740
21. Bastiani, C., and Mendel, J. (2006) *WormBook* 1–25
22. Miller, K. G., Emerson, M. D., McManus, J. R., and Rand, J. B. (2000) *Neuron* **27,** 289–299
23. Miller, K. G., Emerson, M. D., and Rand, J. B. (1999) *Neuron* **24,** 323–333
24. Miller, K. G., and Rand, J. B. (2000) *Genetics* **156,** 1649–1660
25. Afshar, K., Willard, F. S., Colombo, K., Johnston, C. A., McCudden, C. R., Siderovski, D. P., and Gonczy, P. (2004) *Cell* **119,** 219–230
26. Afshar, K., Willard, F. S., Colombo, K., Siderovski, D. P., and Gonczy, P. (2005) *Development* (*Camb.*) **132,** 4449–4459
27. Hess, H. A., Roper, J. C., Grill, S. W., and Koelle, M. R. (2004) *Cell* **119,** 209–218

28. Nipper, R. W., Siller, K. H., Smith, N. R., Doe, C. Q., and Prehoda, K. E. (2007) *Proc. Natl. Acad. Sci. U. S. A.* **104,** 14306–14311
29. Wang, H., Ng, K. H., Qian, H., Siderovski, D. P., Chia, W., and Yu, F. (2005) *Nat. Cell Biol.* **7,** 1091–1098
30. David, N. B., Martin, C. A., Segalen, M., Rosenfeld, F., Schweisguth, F., and Bellaiche, Y. (2005) *Nat. Cell Biol.* **7,** 1083–1090
31. Hampoelz, B., Hoeller, O., Bowman, S. K., Dunican, D., and Knoblich, J. A. (2005) *Nat.Cell Biol.* **7,** 1099–1105
32. Tall, G. G., Krumins, A. M., and Gilman, A. G. (2003) *J. Biol. Chem.* **278,** 8356–8362
33. Nishimura, A., Okamoto, M., Sugawara, Y., Mizuno, N., Yamauchi, J., and Itoh, H. (2006) *Genes Cells* **11,** 487–498
34. Peterson, Y. K., Bernard, M. L., Ma, H., Hazard, S., III, Graber, S. G., and Lanier, S. M. (2000) *J. Biol. Chem.* **275,** 33193–33196
35. Natochin, M., Lester, B., Peterson, Y. K., Bernard, M. L., Lanier, S. M., and Artemyev, N. O. (2000) *J. Biol. Chem.* **275,** 40981–40985
36. Takesono, A., Cismowski, M. J., Ribas, C., Bernard, M., Chung, P., Hazard, S., III, Duzic, E., and Lanier, S. M. (1999) *J. Biol. Chem.* **274,** 33202–33205
37. Bernard, M. L., Peterson, Y. K., Chung, P., Jourdan, J., and Lanier, S. M. (2001) *J. Biol. Chem.* **276,** 1585–1593
38. De Vries, L., Fischer, T., Tronchere, H., Brothers, G. M., Strockbine, B., Siderovski, D. P., and Farquhar, M. G. (2000) *Proc. Natl. Acad. Sci. U. S. A.* **97,** 14364–14369
39. Pizzinat, N., Takesono, A., and Lanier, S. M. (2001) *J. Biol. Chem.* **276,** 16601–16610
40. Adhikari, A., and Sprang, S. R. (2003) *J. Biol. Chem.* **278,** 51825–51832
41. Kimple, R. J., Kimple, M. E., Betts, L., Sondek, J., and Siderovski, D. P. (2002) *Nature* **416,** 878–881
42. Tall, G. G., and Gilman, A. G. (2005) *Proc. Natl. Acad. Sci. U. S. A.* **102,** 16584–16589
43. Du, Q., and Macara, I. G. (2004) *Cell* **119,** 503–516
44. Lee, E., Linder, M. E., and Gilman, A. G. (1994) *Methods Enzymol.* **237,** 146–164
45. Higashijima, T., Ferguson, K. M., Sternweis, P. C., Ross, E. M., Smigel, M. D., and Gilman, A. G. (1987) *J. Biol. Chem.* **262,** 752–756
46. Lanier, S. M. (2004) *Biol. Cell* **96,** 369–372
47. Oldham, W. M., and Hamm, H. E. (2007) *Adv. Protein Chem.* **74,** 67–93
48. Oldham, W. M., and Hamm, H. E. (2008) *Nat. Rev. Mol. Cell Biol.* **9,** 60–71
49. Oldham, W. M., Van Eps, N., Preininger, A. M., Hubbell, W. L., and Hamm, H. E. (2007) *Proc. Natl. Acad. Sci. U. S. A.* **104,** 7927–7932